Geosynthetics - 7th ICG - Delmas, Gourc & Girard (eds) © 2002 Swets & Zeitlinger, Lisse ISBN 90 5809 523 1

Numerical analysis of geosynthetic-reinforced soil subjected to cyclic loads

M.R. MASSIMINO, Department of Civil and Environmental Engineering, University of Catania, Italy

ABSTRACT: Since the 1970's the use of geosynthetics in soil reinforcement has become very widespread, due to their technical and economic benefits in different geotechnical engineering fields. Furthermore, geosynthetic-reinforced soil structures can also be subjected to cyclic loading conditions, as in the case of reinforced embankments and bridge abutments, as well as vibrating foundations. In the present paper a numerical analysis by a non-linear dynamic commercial code is performed in order to investigate the behaviour of geogrid-reinforced soil, to which cyclic loads are transferred by a shallow foundation. Some factors, such as the number and position of the geogrids, are analysed. A comparison with unreinforced soil is also made to highlight the effect of geogrids in reducing foundation settlements and increasing foundation bearing capacity.

1 INTRODUCTION

Geosynthetic-reinforced soil structures have been worldwide utilised in the past, due to their technical and economic benefits in different geotechnical engineering fields, such as retaining structures, slopes, embankments, bridge abutments and foundations. In the last two decades the cyclic loading effects on geosynthetic-reinforced soil behaviour have been considered (Giroud & Noiray, 1981).

Numerous laboratory tests, such as triaxial, direct shear and oedometer tests, have been performed on soil specimens reinforced with geosynthetics to analyse their static and cyclic response (Ashmawy et al., 1999). Recently, theoretical and numerical analyses have been performed to predict the experimental results (Peng et al., 2000). Most of the numerical analyses are related to specimen size, and in the case of full-scale problems to static conditions (Béneito et al., 2000; di Prisco et al., 2001). The cyclic and/or dynamic behaviour of geosynthetic-reinforced soil needs further investigation, above all in terms of numerical analyses.

In the present paper numerical analysis by the finite element commercial ADINA code (Bathe, 2001) is performed to investigate the behaviour of geogrid-reinforced soil, to which cyclic loads are transferred by a shallow foundation. The analysis is performed in plane strain conditions. The soil and foundation are modelled by means of 2-D solid elements, while the geogrids are modelled by means of truss elements. A low frequency sine cyclic load is applied to the foundation.

Some factors, such as the number and position of the geogrids, are investigated. A comparison with unreinforced soil is also made to hightlight the effect of geogrids in reducing foundation settlements and increasing foundation bearing capacity. The results are reported in terms of foundation settlements, critical number of cycles to reach the system failure and axial forces along the geogrids.

2 FEM MODELING

The commercial finite element code ADINA (Automatic Dynamic Incremental Non-linear Analysis) is used in order to investigate the response of a geogrid-reinforced soil supporting a non-embedded rigid foundation subjected to a cyclic vertical load. The soil consists of a deposit, 12.0 m wide and 4.25 m deep. A rigid strip foundation, 2 m wide and 0.50 m thick, rests on the soil surface in a central position.

The soil is reinforced with different layers of geogrids, 4.0 m long. Different geogrid configurations are taken into account: (1) four geogrids located at the depths of 0.25 m, 0.50 m, 0.75 m and 1.00 m respectively; (2) one single geogrid located at the depth of 0.25 m; (3) one single geogrid located at the depth of 0.50 m; (4) one single geogrid located at the depth of 0.75 m; (5) one single geogrid located at the depth of 1.00 m; (6) unreinforced soil. Due to the symmetry of the investigated system, only half the system is taken into account (Fig.1). The analysis is performed in plane strain conditions, utilising 2-D solid elements for the soil and the foundation and truss elements for the geogrids.

The mechanical behaviour of the soil is reproduced by means of an elastic work-hardening plastic isotropic cap constitutive model. In the elastic range the behaviour of the model is governed by the Young modulus E and the Poisson ratio ν. In the plastic range, the behaviour of the model is governed by an isotropic loading function f, which consists of two parts: the

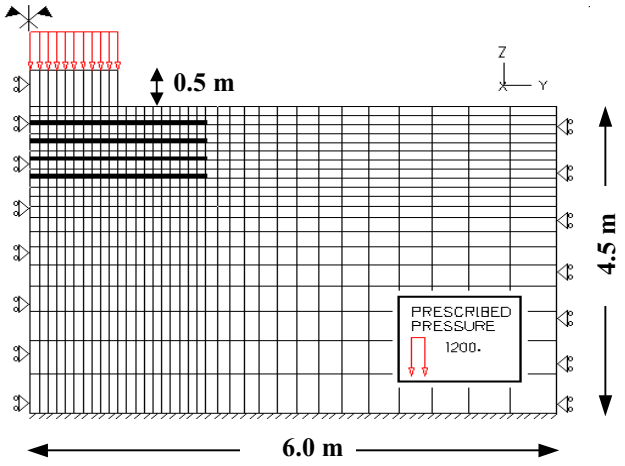

Figure 1. Mesh configuration utilised for the numerical analysis – four geogrid configuration.

Drucker-Prager ultimate failure envelope f_1 and an elliptically shaped strain-hardening cap yield surface f_2, where:

$$f_1 = \sqrt{J_2} - \alpha I_1 - k \quad (1)$$

$$f_2 = \sqrt{J_2} - (1/R)\{[X(\varepsilon_v^p) - L(\varepsilon_v^p)]^2 - [I_1 - L(\varepsilon_v^p)]^2\}^{1/2} \quad (2)$$

being α, k two material constants related to the shear strength angle ϕ and the cohesion c through the following relations:

$$\alpha = (2 \sin\phi) / [\sqrt{3} (3 - \sin\phi)] \quad (3)$$

$$k = (6 c \cos\phi) / [\sqrt{3} (3 - \sin\phi)] \quad (4)$$

Moreover, R is the ratio of the major to the minor axis of the elliptic cap, and $L(\varepsilon_v^p)$ and $X(\varepsilon_v^p)$ define the initial and the final cap position respectively and depend on the volumetric plastic strain ε_v^p. In particular:

$$X(\varepsilon_v^p) = (-1/D) \ln [1 - (\varepsilon_v^p / W)] \quad (5)$$

and

$$X(\varepsilon_v^p) = l(\varepsilon_v^p) + R [\alpha l(\varepsilon_v^p) + k \quad (6)$$

where W and D are two material constants, and $L(\varepsilon_v^p) = l(\varepsilon_v^p)$ if $l(\varepsilon_v^p) > 0$ and $L(\varepsilon_v^p) = 0$ if $l(\varepsilon_v^p) \leq 0$ (Chen & Baladi, 1985). The following values of the soil model parameters are assumed: E_s = 30 MPa, ν_s = 0.3, ρ = 2 kNs^2/m^4, α = 0.19, k = 50, R = 1, W = -0.015 and D = -0.1. The values of the soil stiffness and strength properties are quite low in order to stress the system response in terms of foundation settlements and geogrid axial forces.

The foundation consists of an elastic, linear isotropic material, with E_f = 150 MPa and ν_f = 0.3. Furthermore, PP bi-directional geogrids characterised by the constitutive law curve reported in Fig. 2 are considered.

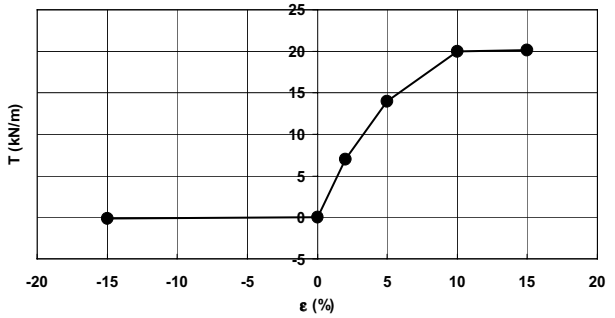

Figure. 2. Constitutive law curve of the utilized geogrids.

As far as the load conditions are concerned, the system is subjected to the mass-proportional load, then a vertical cyclic load is applied to the foundation. This cyclic load is characterised by an angular frequency ω = 180° (f = 0.5 Hz) and a phase angle φ = 180°. The maximum value of the load, equal to 1200 kPa, is fixed considerably high in order to better investigate the system close to its failure condition. A total number of 25 cycles (t = 50 sec) is considered. The analysis is performed in transient dynamic conditions using the Newmark implicit integration method with an automatic time stepping. The Rayleigh damping factors α_{RD} = 0.25 and β_{RD} = 0.025 are also assigned to the system.

3 NUMERICAL RESULTS

Firstly, the effects of geogrid number and position are analysed in terms of maximum foundation settlement, failure condition and axial force absorbed by each geogrid. The configuration with four geogrids is compared with the configuration characterised by one single geogrid at different depths and with the case of unreinforced soil (see paragraph 2). Fig. 3 reports the comparison between the foundation settlement time-history for the case of four geogrid-reinforced soil and that for the case of unreinforced soil. The two time-histories are similar in terms of maximum settlement values, even if bigger settlements are achieved for the unreinforced soil configuration (Fig. 4); but the time-history which regards the unreinforced soil stops at about 29 s due to the system failure, while the time-history concerning the configuration with four geogrids does not stop. Intermediate responses are found for the cases of one single geogrid at different depths (Figs. 4 and 5).

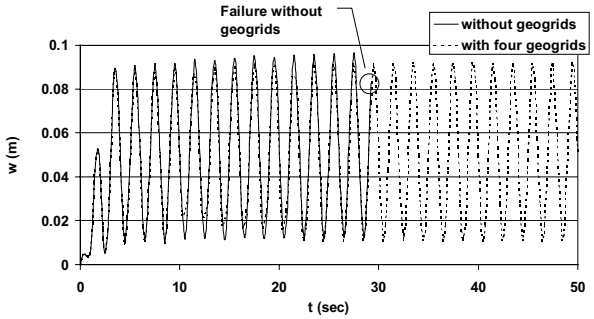

Fig. 3. Foundation settlement time-histories for the configuration with four geogrids and for the unreinforced soil configuration.

In both the two configurations no accumulation of permanent settlements (due to the accumulation of soil plastic strains) versus the load cyclic number can be observed; the absence of soil plastic strain accumulation, generally induced by regular cycles of loading-unloading, depends on the utilised isotropic hardening

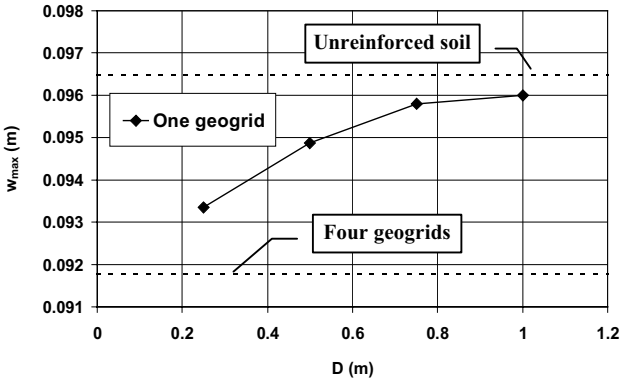

Figure 4. Effects of geogrid depth and number on the maximum value of the foundation settlements.

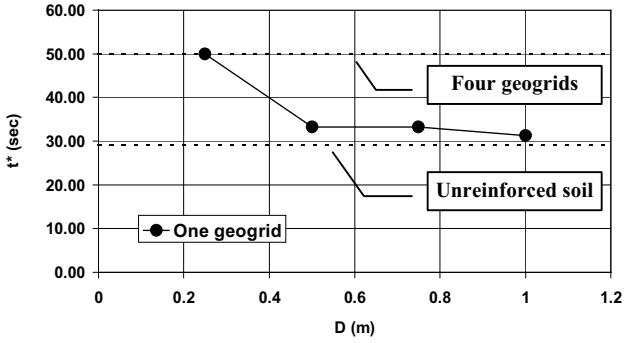

Figure 5. Effects of geogrid depth and number on the cyclic load critical duration before reaching system failure.

soil constitutive models available in commercial codes, which do not allow kinematic hardening plasticity.

Fig. 4 reports the maximum value of the foundation settlements, w_{max}, versus the geogrid depth D, for the cases with one single geogrid at 0.25 m or 0.50 m or 0.75 m or 1.00 m (D/B = 0.125÷0.5). Moreover, the two cases of soil reinforced with four geogrids (see the lower limit) and unreinforced soil (see the upper limit) are shown. It can be seen that for the case of one single geogrid, the nearer the geogrid to the foundation the smaller the foundation settlement. Thus, the configuration with one single geogrid at D = 0.25 m (D/B = 0.125) leads to a value of w_{max} very close to the configuration with four geogrids, on the contrary the configuration with one single geogrid at 1.00 m (D/B = 0.5) leads to a value of w_{max} very close to the unreinforced soil configuration. In any case the values of w_{max} are very high due to the low soil stiffness and the high foundation load, chosen to emphasise the geogrid reinforcement effect.

Fig. 5 reports the duration of the vertical load before the system failure is reached versus the geogrid depth D, for the cases with one single geogrid at 0.25 m or 0.50 m or 0.75 m or 1.00 m (D/B = 0.125÷0.5). Moreover, the two cases of soil reinforced with four geogrids (see the upper limit) and unreinforced soil (see the lower limit) are shown. For the cases of one single geogrid, the nearer the geogrid to the foundation the greater the duration of the vertical load, which can be applied to the soil-foundation system without reaching the system failure. In particular, for the case of one single geogrid at D = 0.25 m, as for the case of four geogrids, no failure occurs. The lowest load duration, equal to about 29 sec (corresponding to about 15 cycles), occurs for the unreinforced soil configuration. Thus, in dynamic and/or cyclic conditions, the capability of reinforced soil to support dynamic and/or cyclic loads greatly depends on the load duration.

As an example Fig. 6 shows the vertical displacement distribution inside the soil and the foundation for the configuration with four geogrids. Fig. 6 is related to the integration time of 49.45 sec, corresponding to the maximum vertical load q = 1200 kPa and a number of cycles of 25.

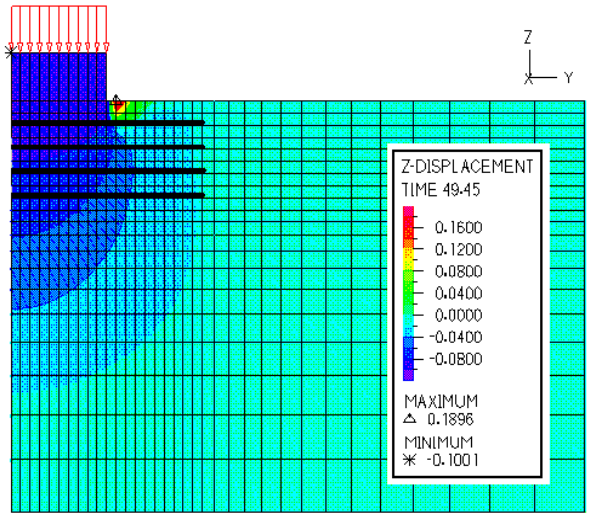

Figure 6. Vertical displacement for the configuration with four geogrids.

The numerical analysis is also focused on the axial force absorbed by the geogrids in the different configurations. Fig. 7 reports the values of the maximum axial force T_{max} reached in the geogrids versus the time t. Curves (A*), (B*), (C*) and (D*) refer to the configuration with four geogrids, in particular curve (A*) refers to the first geogrid located at the depth of 0.25m, curve (B*) refers to the second geogrid located at the depth of 0.50 m, and so on. While curves (A), (B), (C) and (D) refer to the configurations with one single geogrid, so curve (A) refers to one single geogrid at the depth of 0.25 m, curve (B) refers to one single geogrid at the depth of 0.50 m, and so on. Two important results in the geogrid cyclic response can be seen from Fig. 7. Firstly, the value of T_{max} is strongly sensitive to the distance from the foundation: the nearer the geogrid to the foundation, the greater the value of T_{max}, with a difference between the shallowest geogrid and the deepest one of about 120 % for the case with four geogrids and of about 240% for the case with one single geogrid. Secondly, the use of more than one geogrid leads to a significant reduction of T_{max}, with the greatest benefit at a depth

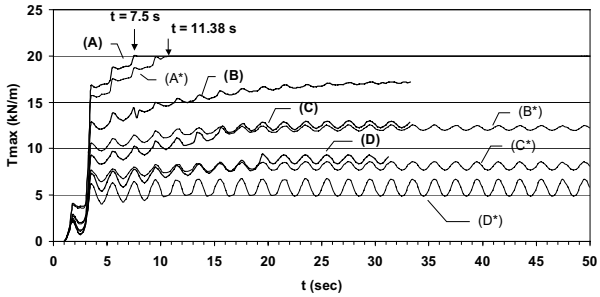

Figure 7. Maximum axial forces reached in the geogrids during the cyclic load application.

of about 0.50 m (D/B = 0.25).

Another important aspect to be investigated is the axial force distribution along the geogrid. This distribution changes during the different cycles: it is quite uniform underneath the foundation and absent outside at the beginning of the cyclic loading (Fig. 8), after a few numbers of cycles a characteristic non-uniform distribution with a marked peak value underneath the end of the foundation can be observed (Fig. 9). This change in the axial force distribution is more evident the nearer the geogrid is to the foundation (Fig. 10a, b, c and d).

4 CONCLUDING REMARKS

Numerical analysis on a geogrid-reinforced soil underneath a shallow foundation subjected to cyclic loading is performed. The main results achieved can be summarised as follows:

- The number and position of the geogrids are very important in order to increase soil-foundation bearing capacity for cyclic loading.
- The main benefit in terms of bearing capacity, is reached for an a-dimensional geogrid depth D/B equal to or less than 0.25, being D the geogrid depth underneath the foundation and B the foundation width.
- The foundation settlements are slightly sensitive to the geogrid number and position, with a maximum reduction of about 5 % comparing unreinforced soil and four geogrid reinforced soil.
- The geogrid maximum axial force, T_{max}, is strongly sensitive to geogrid position, with a difference between the shallowest geogrid and the deepest one up to a value of 240 %.
- The greater the number of geogrids, the less the value of T_{max}, with a maximum benefit for the geogrid at D/B equal to about 0.25.
- The geogrid axial force distribution changes with the cycle numbers, reaching the maximum value underneath the foundation ends after a few number of cycles.
- Future research on geosynthetic-reinforced soil subjected to cyclic and/or dynamic loading should be devoted to implement into numerical codes new soil constitutive models, involving not only isotropic hardening but also kinematic hardening (Gajo & Wood, 1998; 1999). Particular attention should be paid to the effects of cyclic and/or dynamic geosynthetic-soil interface behaviour (Carrubba & Massimino,

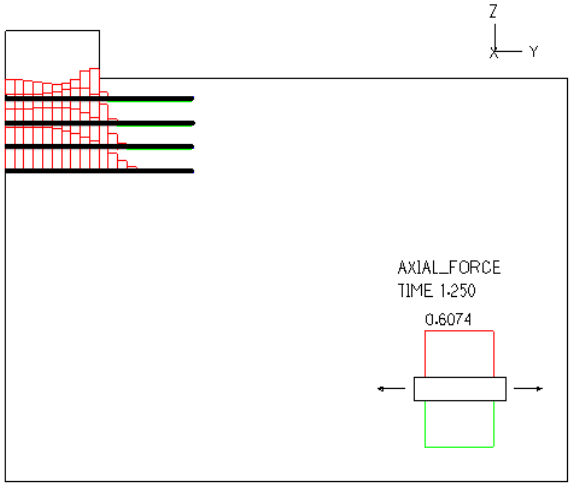

Figure 8. Axial force distribution along the geogrids for the four geogrid reinforced soil configuration, at time t = 1.25 s.

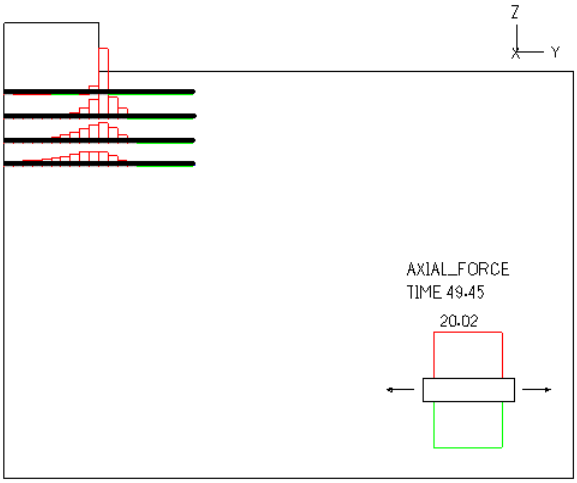

Figure 9. Axial force distribution along the geogrids for the four geogrid reinforced soil configuration, at time t = 49.25 s.

1999; Carrubba et al., 2001). Greater investigation should be focused on the effects of cyclic loading frequency content and peak value, as well as cyclic loading duration.

ACKNOWLEDGE

The Author wishs particularly to say thank you to Prof. M. Maugeri and Prof. P. Carrubba, who have continuosly encouraged her in the study of geosynthetic-reinforced soil behaviour.

References

Ashmawy, A.K., Bourdeau, P.L., Drnevich, V.P. & Dysli, M. 1999. Cyclic response of getextile-reinforced soil. *Soils and foundations Journ.*, 39(1): 43-52.

Bathe, K.J. 2001. ADINA: theory and modelling guide. *Adina R & D*, Watertown, USA.

Bénéito, C., Gotteland, P. & Nancey, A. 2000. *Proc. 2nd Eur. Geosynth. Conf. and Exibition*, Bologna, 16-18 April, 2000.

Carruba, P. & Massimino, M.R. 1999. Geosynthetic interface strenght in dynamic condition. *L'Ingegnere e l'architetto, ANIAI Journ.*, .1/1999 (in Italian).

Carrubba, P., Massimino, M.R. & Maugeri, M. 2001. Dynamic friction of geosynthetic interfaces by shaking table tests. In T.H. Christensen, R. Cossu & R. Stegmann (ed.), *Sardinia 2001, Proc. 8th Int. Waste Management and Landfill Symp.,* S. Margherita di Pula, Cagliari, Italy, 1-5 October 2001, 3: 157-166, CISA: 567-576.

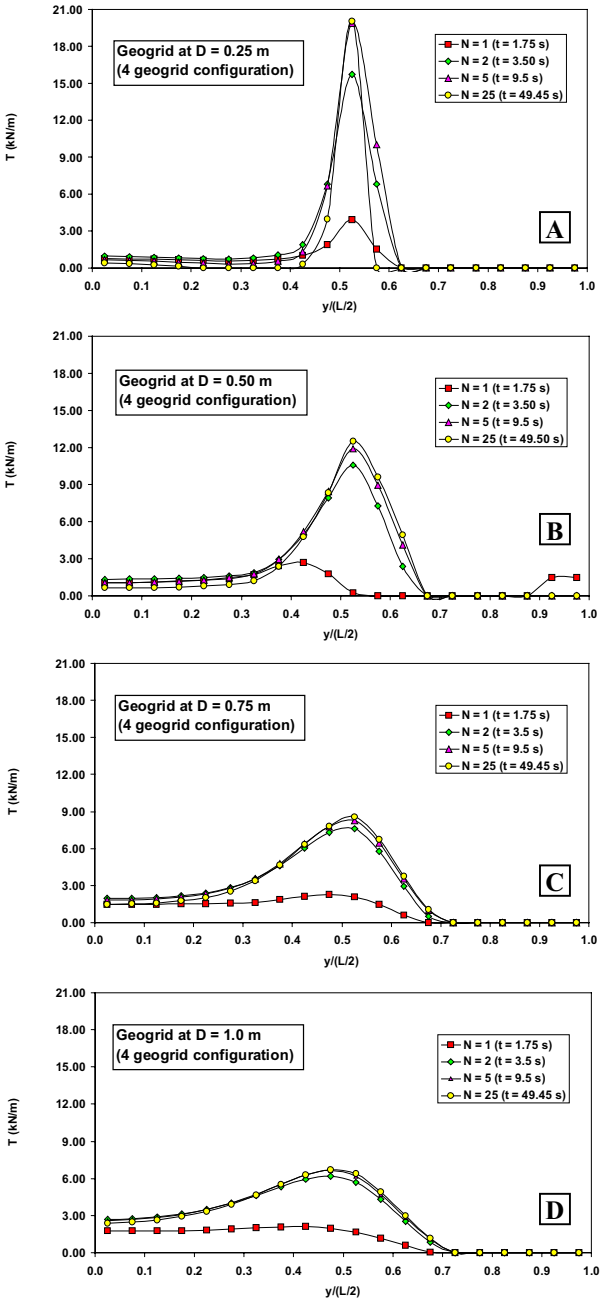

Figure 10. Axial force distribution along the geogrids located at different depths.

Chen, W.F. & Baladi, G.Y. 1985. Soil plasticity: theory and implementation. *Elsevier*, New York, USA.

di Prisco, C., Imposimato, S., Rimordi, P. & Vecchiotti, M. 2001. Numerical analysis of the mechanical behaviour of rigid shallow foundations on geo-reinforced soil strata. In *Landmarks in Earthreinforcement, Proc. Int. Symp. on Earthreinforcements,* H. Ochiai, J. Otani, N. Yasufuku, A. Omine eds., Fukuoka/Kyushu, 14-16 November, 2001.

Gajo, A. & Muir Wood, D. 1998. Numerical analysis of shear stack under dynamic loading. *Proc. 11th Eur. Conf. on Earthq. Engrg.*, Balkema, Rotterdam, 1-12.

Gajo, A. & Muir Wood, D. 1999. A kinematic hardening constitutive model for sands: the multiaxial formulation. *Int. Journ. Num. Anal. Meth. Geomech.*, 23, 925-965.

Giroud, J.P. & Noiray, L. 1981. Geosynthetic-reinforced unpaved road design. *Int. Journ. of Geotech. Engrg., ASCE*, 107(9): 1233-1254.

Peng, F.L., Nozomu, K., Tatsuoka, F., Hirakawa, D. & Tanaka, T. 2000. Plane strain compression behaviour of geogrid-reinforced sand and its numerical analysis.*Soils and Foundations Journ.*, 40(3): 55-74.